Title	On the outage probability of MMSE turbo equalization in frequency-selective Rayleigh fading channels
Author(s)	Grossmann, Marcus; Matsumoto, Tad
Citation	2010 International ITG Workshop on Smart Antennas (WSA): 88-93
Issue Date	2010-02-23
Type	Conference Paper
Text version	publisher
URL	http://hdl.handle.net/10119/9821
Rights	Copyright (C) 2010 IEEE. Reprinted from 2010 International ITG Workshop on Smart Antennas (WSA), 2010, 88-93. This material is posted here with permission of the IEEE. Such permission of the IEEE does not in any way imply IEEE endorsement of any of JAIST's products or services. Internal or personal use of this material is permitted. However, permission to reprint/republish this material for advertising or promotional purposes or for creating new collective works for resale or redistribution must be obtained from the IEEE by writing to pubs-permissions@ieee.org. By choosing to view this document, you agree to all provisions of the copyright laws protecting it.
Description	

On the Outage Probability of MMSE Turbo Equalization in Frequency-Selective Rayleigh Fading Channels

Marcus Grossmann[1], Tad Matsumoto[2]
[1]Institute for Information Technology
Ilmenau University of Technology, Germany
[2]Japan Advanced Institute of Science and Technology, Japan
Email: marcus.grossmann@tu-ilmenau.de, matumoto@jaist.ac.jp

***Abstract*— We analyze the outage probability of frequency domain minimum mean squared error turbo equalization over frequency-selective Rayleigh fading channels with exponential delay power profile. A correlation chart analysis is used to evaluate the convergence property of the iterative system. Based on the convergence characteristic of the equalizer and decoder, we derive a closed form approximation to the outage probability of the turbo equalizer. Specifically, an upper bounding technique and a central limit theorem are used to show that the outage probability is well approximated by a sum of complementary Gaussian error functions. Numerical results of outage probability simulations of the turbo equalizer in channels with different delay power profiles are presented to demonstrate the accuracy of the proposed method.**

I. Introduction

Turbo equalization [1]-[4] is one of the most promising techniques, without requiring excessive computational complexity, for coded transmissions over frequency-selective fading channels. The complexity advantage of turbo equalization is due to the separation of channel equalization and decoding into two basic soft-input soft-output (SfiSfo) processing components, while such high performance can be achieved by exchanging soft information between the SfiSfo components in an iterative manner. Turbo equalization was originally proposed in [1], utilizing a maximum a posteriori probability (MAP) algorithm for iterative processing in frequency-selective fading channels. However, because of its exponentially increasing complexity, the MAP-based equalizer is only practical for simple modulation formats, like binary phase shift keying (BPSK), and for channels with few multipath components. In [2], the optimal MAP algorithm has been replaced by a low-cost alternative based on the soft canceling (SC) and minimum mean-squared error (MMSE) principle. The SC-MMSE filtering approach in [2], originally proposed for the detection of random coded code-division multiple-access (CDMA) signals, has been applied to channel equalization in [3]. In [4], a turbo equalizer for single carrier transmission over broadband channels is proposed that performs the MMSE filtering in frequency domain (FD). Due to using the computationally efficient fast Fourier transform, the SC FD-MMSE equalizer in [4] has much lower complexity than its time-domain counterpart presented in [3].

In this paper, we analyze the performance of SC FD-MMSE turbo equalization in frequency-selective Rayleigh fading channels with exponential delay power profile. Specifically, we focus on the outage probability, which is defined by the probability of unsuccessful convergence of the equalizer, given random channel realizations.

We first provide a correlation chart analysis [5], similar to the well known extrinsic information transfer (EXIT) chart analysis [6], to evaluate the convergence property of the turbo system. In fact, as shown in [7], the correlation chart method provides us with an analytical expression describing the convergence property of the equalizer. We then use the correlation functions of the equalizer and decoder to derive a closed-form approximation on the outage probability. In particular, using a union bounding technique and a central limit theorem, we show that the outage probability is well approximated by a sum of complementary Gaussian error functions.

II. System Model and Turbo Equalization

Consider a single carrier cyclic prefix assisted block-transmission wireless communication system. The transmission scheme is based on bit interleaved coded modulation (BICM), where the information bit sequence is encoded by a rate-r_c binary encoder, randomly bit-interleaved, BPSK modulated, and grouped into N $(n = 1, .., N)$ blocks

$$\mathbf{b}(n) \equiv \left[b_0(n), ..., b_q(n), ..., b_{Q-1}(n)\right]^T \quad (1)$$

that are transmitted over the frequency-selective fading channel.

The channel $\mathbf{h} \equiv \left[h(0), ..., h(L-1)\right]^T$ is composed of L taps and assumed to be constant during the transmission of one frame (comprised of N blocks), but varying randomly and independently frame-by-frame. Thus, we consider a slowly time-varying fading channel. We also assume that the L channel gains are perfectly known at the receiver.

Employing a cyclic prefix of length $P = L - 1$ to each transmit block, the received signals can be expressed as

$$\mathbf{r}(n) = \mathbf{H}\mathbf{b}(n) + \mathbf{v}(n), n = 1, .., N, \quad (2)$$

978-1-4244-6072-4/10/$26.00

where $\mathbf{H} = \mathrm{circ}_Q\{\mathbf{h}\}$ is the circulant channel matrix of size $Q \times Q$, and $\mathbf{v}(n) \sim \mathcal{CN}(\mathbf{0}, \sigma^2\mathbf{I})$ is the additive white Gaussian noise (AWGN). Note that $\mathbf{H}$ may be decomposed into a diagonal matrix $\boldsymbol{\Xi}$ by the Fourier matrix,

$$\mathbf{H} = \mathbf{F}^H \boldsymbol{\Xi} \mathbf{F}, \tag{3}$$

where $\mathbf{F}$ denotes the Fourier matrix of size Q, whose (l, j)-th element is given by $Q^{-\frac{1}{2}} e^{-i\frac{2\pi}{Q}lj}$, $0 \leq l, j \leq Q-1$, and $\boldsymbol{\Xi} = \mathrm{diag}\{\boldsymbol{\tau}\}$ is the FD channel matrix with $\boldsymbol{\tau}$ being a vector comprising the FD channel coefficients, i.e., $\boldsymbol{\tau} = \mathbf{F}^H\tilde{\mathbf{h}}$ with $\tilde{\mathbf{h}} = [\mathbf{h}^T, \mathbf{0}_{1\times(Q-L-1)}]^T$. At the receiver side, iterative processing for joint equalization and decoding is performed. The receiver consists of a SC FD-MMSE equalizer and a single-user a posteriori probability decoder. Within the iterative processing, *extrinsic* log likelihood ratios (LLRs) of the coded bits are exchanged between the equalizer and decoder, following the turbo principle [2]. Inputs to the equalizer are the received signals $\mathbf{r}(n)$ and the *a priori* LLR sequences

$$\boldsymbol{\zeta}(n) \equiv \big[\zeta_0(n), ..., \zeta_q(n), ..., \zeta_{Q-1}(n)\big]^T \text{ for all } n, \tag{4}$$

where $\zeta_q(n) \equiv \log\Big(\mathrm{Prob}\big(b_q(n) = +1\big)/\mathrm{Prob}\big(b_q(n) = -1\big)\Big)$. The equalizer first generates an estimate of the received signal $\mathbf{r}(n)$ and then subtracts it from $\mathbf{r}(n)$, yielding the residual:

$$\tilde{\mathbf{r}}(n) = \mathbf{r}(n) - \mathbf{H}\bar{\mathbf{b}}(n) \tag{5}$$

where $\bar{\mathbf{b}}(n) = [\bar{b}_0(n), ..., \bar{b}_{Q-1}(n)]^T$ is a vector comprising the expected values of the elements in $\mathbf{b}(n)$, i.e.,

$$\bar{\mathbf{b}}(n) = \tanh\Big(\frac{\boldsymbol{\zeta}(n)}{2}\Big). \tag{6}$$

After the residual $\tilde{\mathbf{r}}(n)$ is calculated, linear adaptive FD filtering is performed to extract the desired signal components $\mathbf{b}(n)$ as [3] [4]

$$\mathbf{z}(n) = (1 + \gamma\varphi)^{-1} \left(\gamma\bar{\mathbf{b}}(n) + \mathbf{F}^H\boldsymbol{\Psi}\mathbf{F}\tilde{\mathbf{r}}(n)\right), \tag{7}$$

where $\mathbf{z}(n) = [z_0(n), ..., z_q(n), ..., z_{Q-1}(n)]^T$, $\varphi = \frac{1}{QN}\sum_{n=1}^{N} \bar{\mathbf{b}}^T(n)\bar{\mathbf{b}}(n)$ is the mean energy of the symbol estimates in $\bar{\mathbf{b}}(n)$, $\boldsymbol{\Psi} = \boldsymbol{\Xi}^H\left[(1-\varphi)\boldsymbol{\Xi}\boldsymbol{\Xi}^H + \sigma^2\mathbf{I}\right]^{-1}$ is the frequency domain filter, and $\gamma = (1/Q)\mathrm{Trace}\{\boldsymbol{\Psi}\boldsymbol{\Xi}\}$. The equalizer then computes the extrinsic LLR for each transmitted bit $b_q(n)$ as

$$\lambda_q(n) \equiv \log\left(\frac{\mathrm{Prob}\big(z_q(n)|b_q(n) = +1\big)}{\mathrm{Prob}\big(z_q(n)|b_q(n) = -1\big)}\right). \tag{8}$$

Following [3], we may approximate $z_q(n)$ by an equivalent AWGN channel having $b_q(n)$ as its input, so that

$$\mathrm{Prob}\left(z_q(n)|b_q(n) = b\right) \sim \mathcal{N}(\mu_b b, \sigma_b^2), b \in \{\pm 1\}, \tag{9}$$

where $\mu_b = \gamma/(1+\gamma\varphi)$, and $\sigma_b^2 = \mu_b(1-\mu_b)$.

Note that during the first iteration of turbo equalization, $\zeta_q(n)$ is zero for all n, q, and later on $\zeta_q(n)$ is provided via the interleaver in the form of extrinsic LLRs of the decoder.

A. Channel Model and Correlation Properties

We consider Rayleigh block-fading channels, where the channel coefficients $h(l)$, $l = 0, ..., L-1$ are assumed to be independent and identically distributed (i.i.d) circulary-symmetric complex Gaussian random variables. Furthermore, we presume that the delay autocorrelation function of the channel $\mathbf{h}$ is described by an exponential delay power profile with normalized root mean square (rms) delay τ_d,

$$p(l) = \upsilon \exp\Big(-\frac{l}{\tau_d}\Big), \text{ for } l = 0, ..., L-1, \tag{10}$$

where $\upsilon = L/\sum_l p(l)$ is a normalization constant.

Let us write the q_1th and q_2th FD channel coefficients as

$$\begin{aligned}\tau_{q_1} &= \tau_{c,q_1} + i\tau_{s,q_1},\\ \tau_{q_2} &= \tau_{c,q_2} + i\tau_{s,q_2}.\end{aligned} \tag{11}$$

In (11), the random variables τ_{c,q_1}, τ_{s,q_1}, τ_{c,q_2} and τ_{s,q_2} are identically zero-mean Gaussian distributed with variance $\eta/2$, where $\eta = \frac{L}{Q}$. Assume that, as L and Q increase, the normalized frequency separation $\Delta f \equiv \tau_d/Q$ remains fixed. Following [8], we then may write the cross-correlations of the random variables in (11) for $L, Q \to \infty$ as

$$\begin{aligned}&\mathrm{E}[\tau_{c,q_1}\tau_{s,q_1}] = \mathrm{E}[\tau_{c,q_2}\tau_{s,q_2}] = 0\\ &\mathrm{E}[\tau_{c,q_1}\tau_{c,q_2}] = \mathrm{E}[\tau_{s,q_1}\tau_{s,q_2}] = \frac{\eta/2}{1+(2\pi\Delta f\Delta q)^2}\\ &\mathrm{E}[\tau_{c,q_1}\tau_{s,q_2}] = -\mathrm{E}[\tau_{c,q_2}\tau_{s,q_1}] = -\frac{\eta\pi\Delta f\Delta q}{1+(2\pi\Delta f\Delta q)^2},\end{aligned} \tag{12}$$

where $\Delta q = |q_1 - q_2|$. From (12), we observe that $(\tau_{c,q_1}, \tau_{s,q_1})$ and $(\tau_{c,q_2}, \tau_{s,q_2})$ form a *circular pair* [9]. Therefore, the exponential distributed FD channel gains $\kappa_q = \tau_{c,q}^2 + \tau_{s,q}^2$ with mean η and variance η^2 for all $q = 0, .., Q-1$, have the correlation coefficient [9]

$$\delta_{\Delta q} = \frac{1}{1+(2\pi\Delta f\Delta q)^2}. \tag{13}$$

III. Convergence Characteristic of the Turbo Equalizer

In this section, the correlation chart analysis [5] is used to study the convergence characteristic of the SC FD-MMSE turbo equalizer.

Let $\varphi_e \equiv \mathrm{E}[b_q(n)a_q(n)]$ be the correlation between the true binary transmit signal $b_q(n)$ and the MMSE estimate $a_q(n) \equiv E[b_q(n)\,|\lambda_q(n)] = \tanh\big((1/2)\lambda_q(n)\big)$ of $b_q(n)$ given $\lambda_q(n)$. Following [6], we model $(1/2)b_q(n)\lambda_q(n)$ as i.i.d. Gaussian random variables. We assume that the *symmetry condition* [6] for all LLR messages is satisfied, so that $p(x) = p(-x)\exp(x)$, where $p(x)$ is the probability density function (PDF) of an LLR message. By enforcing this condition on the random variables $(1/2)b_q(n)\lambda_q(n)$, we obtain

$$\mathrm{E}\Big[\frac{1}{2}b_q(n)\lambda_q(n)\Big] = \mathrm{Var}\Big[\frac{1}{2}b_q(n)\lambda_q(n)\Big] = \frac{2\mu_b}{1-\mu_b}. \tag{14}$$

Similarly, let $\varphi_d \equiv \mathrm{E}[b_q(n)c_q(n)]$ be the correlation between $b_q(n)$ and $c_q(n) = \tanh\big((1/2)\zeta_q(n)\big)$. Then using (7), we can express the effective signal-to-noise ratio (SNR) Ψ at the equalizer output as

$$\begin{aligned}\Psi(\varphi_d) &= \frac{2\mu_b}{1-\mu_b} \\ &= \frac{2\gamma}{1-\gamma(1-\varphi_d)} \\ &= \frac{2}{1-\varphi_d}\left[Q\left(\sum_{q=0}^{Q-1}\frac{1}{1+\rho\kappa_q}\right)^{-1}-1\right], \qquad (15)\end{aligned}$$

where $\rho \equiv (1-\varphi_d)/\sigma^2$. Under the Gaussian assumption, the correlation φ_e is then given by

$$\begin{aligned}\varphi_e &= \frac{1}{\sqrt{2\pi}}\int_{-\infty}^{\infty}\tanh\left(z\sqrt{\Psi(\varphi_d)}+\Psi(\varphi_d)\right)e^{\frac{-z^2}{2}}\mathrm{d}z, \qquad (16)\\ &\equiv \phi(\Psi(\varphi_d)), \qquad (17)\\ &\equiv f_e(\varphi_d), \qquad (18)\end{aligned}$$

where we have defined $\phi(x) = \frac{1}{\sqrt{2\pi}}\int_{-\infty}^{\infty}\tanh\left(z\sqrt{x}+x\right)e^{\frac{-z^2}{2}}\mathrm{d}z$. The function $f_e(.)$ in (18) is referred to as the correlation characteristic of the equalizer in what follows. Similarly, the correlation φ_d can be expressed as

$$\varphi_d = f_d(\varphi_e), \qquad (19)$$

where $f_d(.)$ is denoted as the correlation characteristic of the decoder. We obtain f_d by a Monte Carlo method, as described in [5].

With the definitions in (18) and (19), the convergence behavior of the turbo equalizer can now be analyzed by evaluating the correlation sequence $\{\varphi_e^{(l)}, \varphi_d^{(l)}\}$, $l = 0, ..., T$, over T iterations between the equalizer and decoder, generated by

$$\begin{aligned}\varphi_e^{(l)} &= f_e(\varphi_d^{(l)}) \text{ with } \varphi_d^{(0)} = 0, \qquad (20)\\ \varphi_d^{(l+1)} &= f_d(\varphi_e^{(l)}). \qquad (21)\end{aligned}$$

The functions $f_e(.)$ and $f_d(.)$ are bounded and monotonically increasing in φ_d and φ_e, respectively. Thus, the sequence $\{\varphi_e^{(l)}, \varphi_d^{(l)}\}$ convergences asymptotically to fixed values $\{\tilde{\varphi}_e, \tilde{\varphi}_d\}$ with $\tilde{\varphi}_e = \lim_{l\to\infty}\varphi_e^{(l)}$ and $\tilde{\varphi}_d = \lim_{l\to\infty}\varphi_d^{(l)}$, for $T \to \infty$. The function $f_e(.)$ is shown for an example snapshot in Fig. 1. Also shown is the inverse function of $f_d(.)$, denoted as $f_{I,d}(.)$, and the decoding trajectory that visualizes the correlation exchange between the equalizer and decoder. The function $f_{I,d}(.)$ has been calculated for a rate-$1/2$ memory-three convolutional code.

Convergence of turbo equalization is achieved when $\varphi_d^{(l)}$ attains the maximum value $\tilde{\varphi}_d = 1$. Obviously, this is possible for T being sufficiently large, if the following constraint holds:

$$f_e(\varphi_d) > f_{I,d}(\varphi_d), \ \forall\varphi_d \in [0,1). \qquad (22)$$

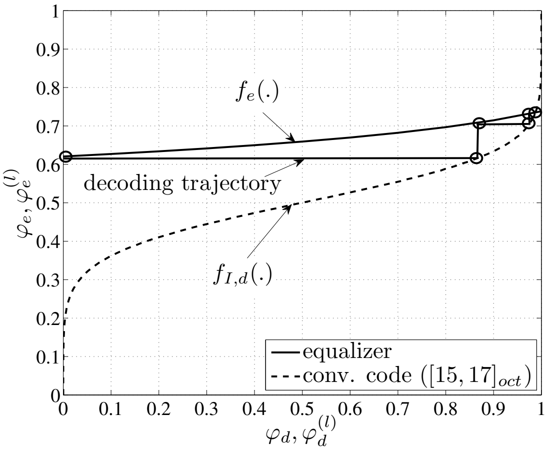

Fig. 1. Equalizer and decoder correlation characteristics for a random channel realization ($L = 32$, $\tau_d = 5$) at $E_b/N_0 = 3$ dB.

IV. Outage Probability Analysis

The turbo equalizer is in outage if for the specific channel realization $\tilde{\varphi}_d < 1$. Hence, an outage event $\mathcal{O}$ occurs when $f_e(\varphi_d) \le f_{I,d}(\varphi_d)$ for at least one value of $\varphi_d \in [0,1)$. Thus, we can define the outage probability of the turbo equalizer as

$$\text{Prob}(\mathcal{O}) \equiv \text{Prob}\left(f_e(\varphi_d) \le f_{I,d}(\varphi_d), \ \exists\varphi_d \in [0,1)\right). \qquad (23)$$

A direct evaluation of the constraint $f_e(\varphi_d) \le f_{I,d}(\varphi_d)$ in (23) on the continuous interval $\varphi_d \in [0,1)$ is computationally intractable. Therefore, we proceed by imposing the constraint on a discrete set of D values $\{\varphi_{d,k}\}$, $k = 1, .., D$. Then, using the union bound [13], we find an approximate upper bound on (23) as

$$\text{Prob}(\mathcal{O}) \le \sum_{k=1}^{D}\text{Prob}\left(f_e(\varphi_{d,k}) \le f_{I,d}(\varphi_{d,k})\right). \qquad (24)$$

Using (17) and (15), we can write (24) as

$$\begin{aligned}\text{Prob}(\mathcal{O}) &\le \sum_{k=1}^{D}\text{Prob}\left(\phi(\Psi(\varphi_{d,k})) \le f_{I,d}(\varphi_{d,k})\right) \\ &= \sum_{k=1}^{D}\text{Prob}\left(\frac{1}{Q}\sum_{q=0}^{Q-1}\frac{1}{1+\rho_k\kappa_q} > A_k\right), \qquad (25)\end{aligned}$$

where

$$\begin{aligned}\rho_k &= (1-\varphi_{d,k})/\sigma^2, \qquad (26)\\ A_k &= \frac{2}{(1-\varphi_{d,k})\phi_I(f_{I,d}(\varphi_{d,k}))+2} \qquad (27)\end{aligned}$$

with $\phi_I(.)$ being the inverse function of $\phi(.)$. For convenience, we define

$$\begin{aligned}S_k &\equiv \frac{1}{Q}\sum_{q=0}^{Q-1}\frac{1}{1+\rho_k\kappa_q} \\ &= \frac{1}{Q}\sum_{q=0}^{Q-1}c_k(\kappa_q) = \frac{1}{Q}\sum_{q=0}^{Q-1}s_k\left(\tau_{c,q}, \tau_{s,q}\right), \qquad (28)\end{aligned}$$

where $c_k(\kappa_q) = s_k\big(\tau_{c,q}, \tau_{s,q}\big) \equiv \frac{1}{1+\rho_k\kappa_q}$. Exact calculation of the distribution of S_k in (28) is not easy, since as shown in Section II-A, the FD channel coefficients κ_q are correlated with order $1/(\Delta q)^2$. We use a theorem from *Arcones* [10] to show that S_k is asymptotically Gaussian distributed. Note that this theorem has also been adapted in [11] to calculate the capacity of OFDM systems.

We state *Arcones*' theorem below. A proof of it can be found in [10].

Theorem 1: Let $\{\mathbf{X}_j\}$, $\mathbf{X}_j \equiv \big[X_j^{(1)}, ..., X_j^{(d)}\big]^T$, $0 \le j < \infty$ be a stationary zero-mean sequence of Gaussian random vectors in $\mathbb{R}^d$ with covariance function

$$r^{(i,l)}(k) = \mathrm{E}\big[X_m^{(i)} X_{m+k}^{(l)}\big] \tag{29}$$

for $k \in \mathbb{Z}$, $0 \le m < \infty$ and $m + k \ge 0$. Let $f : \mathbb{R}^d \to \mathbb{R}$ be a real-valued function with Hermite rank $\nu(f)$ such that $1 \le \nu(f) < \infty$. Suppose that

$$\sum_{k=-\infty}^{\infty} \Big| r^{(i,l)}(k) \Big|^{\nu(f)} < \infty \tag{30}$$

for $1 \le i, l \le d$. Then, as Q tends to infinite

$$\frac{1}{\sqrt{Q}} \sum_{j=0}^{Q-1} \big(f(\mathbf{X}_j) - \mathrm{E}[f(\mathbf{X}_j)]\big) \xrightarrow{d} \mathcal{N}\Big(0, \sigma^2_{\{\mathbf{X}_j\}}\Big), \tag{31}$$

where $\xrightarrow{d}$ denotes convergence in distribution, and

$$\begin{aligned} \sigma^2_{\{\mathbf{X}_j\}} &= \mathrm{E}\Big[\big(f(\mathbf{X}_0) - \mathrm{E}[f(\mathbf{X}_0)]\big)^2\Big] \\ &+ 2\sum_{j=0}^{\infty} \mathrm{E}\Big[\big(f(\mathbf{X}_0) - \mathrm{E}[f(\mathbf{X}_0)]\big)\big(f(\mathbf{X}_k) - \mathrm{E}[f(\mathbf{X}_k)]\big)\Big]. \end{aligned} \tag{32}$$

We apply Theorem 1 to the sequence of Gaussian FD channel coefficients $\{\mathbf{X}_q\}$, $0 \le q \le Q-1$ with $\mathbf{X}_q = [\tau_{c,q}, \tau_{s,q}]^T$, $d = 2$. In [11], it was shown that for a zero-mean $d = 2$ stationary Gaussian sequence with the correlation properties described in (12), the condition in (30) is satisfied if the Hermite rank of the function $f(.)$ is at least two. Let $f(\mathbf{X}_q) = s_k(\tau_{c,q}, \tau_{s,q})$. In Appendix A, we show that $s_k(.)$ has Hermite rank $\nu(s_k) \ge 2$. Requirement (30) is then satisfied, so that

$$\begin{aligned} \frac{1}{\sqrt{Q}} \sum_{q=0}^{Q-1} \Big(s_k\big(\tau_{c,q}, \tau_{s,q}\big) - \mathrm{E}\big[s_k\big(\tau_{c,q}, \tau_{s,q}\big)\big]\Big) \\ \xrightarrow{d} \mathcal{N}\Big(0, \sigma^2_{\{s_k\}}\Big). \end{aligned} \tag{33}$$

Therefore, for large finite Q, the distribution of S_k in (28) may be approximated by a Gaussian random variable having mean $\mu_{S_k} = \mathrm{E}\big[c_k(\kappa_q)\big]$ and variance

$$\begin{aligned} \sigma^2_{S_k} &= \mathrm{Var}\big[S_k\big] \\ &= \frac{1}{Q}\mathrm{Var}\big[c_k(\kappa_q)\big] + \frac{2}{Q^2}\sum_{j=1}^{Q-1}(Q-j)\mathrm{Cov}\big[c_k(\kappa_0), c_k(\kappa_j)\big]. \end{aligned} \tag{34}$$

The quantities $\mathrm{E}\big[c_k(\kappa_q)\big]$ and $\mathrm{Var}\big[c_k(\kappa_q)\big]$ can be calculated as

$$\begin{aligned} \mathrm{E}\big[c_k(\kappa_q)\big] &= \int_0^\infty \frac{1}{1+\rho_k\kappa_q} p(\kappa_q)\mathrm{d}\kappa_q, \\ \mathrm{Var}\big[c_k(\kappa_q)\big] &= \int_0^\infty \left(\frac{1}{1+\rho_k\kappa_q} - \mathrm{E}\big[c_k(\kappa_q)\big]\right)^2 p(\kappa_q)\mathrm{d}\kappa_q, \end{aligned}$$

where $p(\kappa_q)$ is the PDF of κ_q. Since κ_q is exponential distributed, $p(\kappa_q) = 1/\eta\exp(-\kappa_q/\eta)$. Therefore, $\mathrm{E}\big[c_k(\kappa_q)\big]$ and $\mathrm{Var}\big[c_k(\kappa_q)\big]$ may be written as

$$\mathrm{E}\big[c_k(\kappa_q)\big] = \frac{\eta}{\rho_k} e^{\frac{\eta}{\rho_k}} E_1\Big(\frac{\eta}{\rho_k}\Big), \tag{35}$$

$$\mathrm{Var}\big[c_k(\kappa_q)\big] = \frac{\eta}{\rho_k}\Big[1 - \tfrac{\eta}{\rho_k} e^{\frac{\eta}{\rho_k}} E_1\Big(\tfrac{\eta}{\rho_k}\Big)\Big(1 + e^{\frac{\eta}{\rho_k}} E_1\big(\tfrac{\eta}{\rho_k}\big)\Big)\Big], \tag{36}$$

where $E_1(x) = \int_x^\infty e^{-t}/t\mathrm{d}t$ denotes the exponential integral function. A derivation of $\mathrm{Cov}\big[c_k(\kappa_0), c_k(\kappa_j)\big]$ in (34) is given in Appendix B. Using (34) and (35), we may express (24) as

$$\begin{aligned} \mathrm{Prob}(\mathcal{O}) &\le \sum_{k=1}^{D} \frac{1}{\sqrt{2\pi}\sigma_{S_k}} \int_{A_k}^{\infty} \exp\Big[\frac{-\big(x-\mu_{S_k}\big)^2}{2\sigma^2_{S_k}}\Big]\mathrm{d}x \\ &= \frac{1}{2}\sum_{k=1}^{D} \mathrm{erfc}\Big(\frac{A_k - \mu_{S_k}}{\sqrt{2}\sigma_{S_k}}\Big), \end{aligned} \tag{37}$$

where $\mathrm{erfc}(x) = \frac{2}{\sqrt{\pi}}\int_x^\infty e^{-t^2}\mathrm{d}t$ is the complementary Gaussian error function.

V. Numerical Results

In this section, we provide results of simulations for the outage performance of the SC FD-MMSE turbo equalizer and the union bounding technique from Section IV. We consider a single carrier CP-assisted block-transmission system with each block having $Q = 128$ BPSK symbols. The binary encoder at the transmitter is a serially concatenated convolutional code (SCCC), consisting either of a rate-$1/2$ or rate-$3/4$ outer encoder and a recursive rate-1 inner encoder. The systematic rate-$1/2$, memory-4 code is defined by the generator $(g_r, g_0) = (23, 35)$, where g_r denotes the feedback polynomial. The higher rate-$3/4$ code is obtained by puncturing, as specified in [14]. The recursive rate-1 inner encoder has generator polynomials $(g_r, g_0) = (3, 2)$. We evaluate the outage performance for Rayleigh block-fading channels with $L = 32$ path components and exponential delay power profiles with $\tau_d = 5$ and $\tau_d = 8$. The length of a frame is fixed to $NQ = 8192$ BPSK symbols, and thus the channel is assumed to be constant over $N = 64$ transmitted blocks. The CP length is set to $P = 31$. The turbo equalizer performs 10 iterations between the equalizer and the SCCC decoder, and 20 iterations between the inner and outer channel decoder. For the calculation of the union bound in (37), the constraint in (24) is computed on a grid of $D = 5$ points, such that $\varphi_{d,1} = 0.01$, $\varphi_{d,2} = 0.3$, $\varphi_{d,3} = 0.6$, $\varphi_{d,4} = 0.9$, and $\varphi_{d,5} = 0.99$.

The outage performances of the SC FD-MMSE turbo equalizer and the union bound in (37) for transmissions over

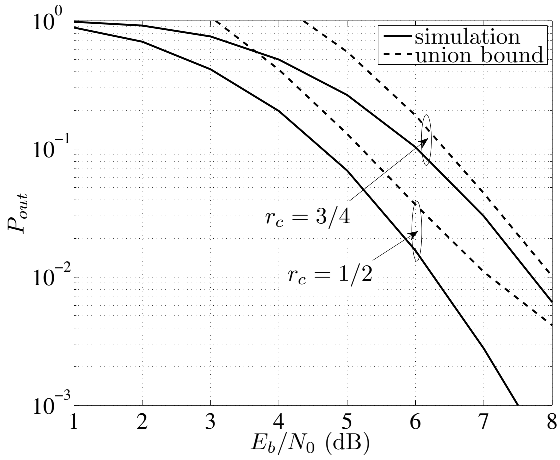

(a)

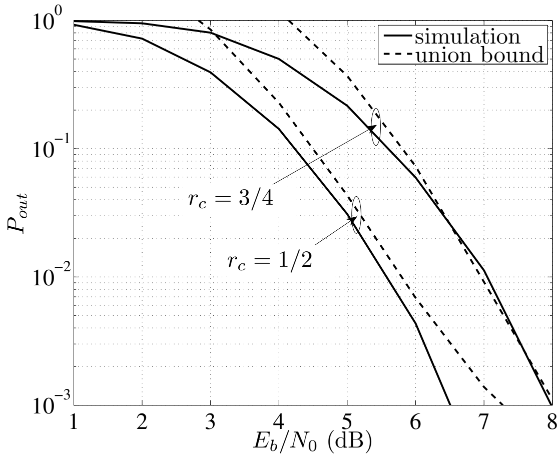

(b)

Fig. 2. Outage probability and union bound of the SC FD-MMSE turbo equalizer utilizing SCCCs with rates $r = 1/2$ and $3/4$ for $L = 32$-tap Rayleigh fading channel having an exponential delay power profile with normalized rms delay (a) $\tau_d = 5$ and (b) $\tau_d = 8$.

$\tau_d = 5$ and $\tau_d = 8$ channels are shown in Fig. 2 (a) and 2 (b), respectively. The outage probabilities (P_{out}) have been computed by averaging over 50000 random channel realizations. We observe that the performance improves with increasing values of rms delay τ_d due to increasing channel diversity. Also, observe that we obtain a reasonable analytical approximation of the outage probability using the proposed union bounding technique for all configurations, where the performance gap between simulation and bound is smaller than $E_b/N_0 = 0.8$ dB for $P_{out} = 10^{-2}$.

VI. Conclusion

We have considered the performance of FD SC-MMSE turbo equalization over frequency-selective Rayleigh fading channels with exponential delay power profile. A correlation analysis has been provided to evaluate the convergence property of the turbo equalization system. Using the correlation functions of the equalizer and decoder, we have derived a closed form expression to the outage probability of the turbo equalizer. Numerical results show that the technique presented in this paper yields a reasonable approximation of the outage performance of the FD SC-MMSE turbo equalizer in frequency-selective Rayleigh fading channels.

References

[1] C. Douillard, et al., "Iterative correction of intersymbol interference: Turbo equalization," *European Trans. Telecomm.*, vol. 6, pp. 507-511, Sept. 1995.

[2] X. Wang, and H. V. Poor, "Iterative (turbo) soft interference cancellation and decoding for coded CDMA," *IEEE Trans. Commun.*, vol. 47, pp. 1046-10611, July 1999.

[3] M. Tüchler, and J. Hagenauer, "Turbo equalization: principles and new results," *IEEE Trans. Commun.*, vol. 50, pp. 754-767, May 2002

[4] K. Kansanen, and T. Matsumoto, "An analytical method for MMSE MIMO turbo equalizer EXIT chart computation," *IEEE Trans. Wireless Commun.*, vol. 6, no. 1, pp. 59-63, Jan. 2007.

[5] J. Choi, "A Correlation Based Analysis for Approximate MAP Detectors and Iterative Receivers," *IEEE Trans. Wireless Commun.*, vol. 6, no. 5, pp. 1764-1773, May 2007.

[6] S. ten Brink, "Convergence behavior of iteratively decoded parallel concatenated codes," *IEEE Trans. Commun.*, vol. 49, pp. 1727-1737, Oct. 2001.

[7] M. Grossmann, and T. Matsumoto, "Nonlinear Frequency Domain MMSE Turbo Equalization using Probabilistic Data Association," *IEEE Commun. Letters*, vol. 12, pp. 295-297, April 2008.

[8] W. C. Jakes, "Microwave Mobile Communications,"*New York, NY: IEEE Press*, 1994.

[9] R. K. Malik, "On multivariate Rayleigh and exponential distributions," *IEEE Trans. Inf. Theory*, vol. 49, no. 6, pp. 1499-1515, Jun. 2003.

[10] M. A. Arcones, "Limit theorems for nonlinear functionals of a stationary Gaussian sequence of vectors," *The Annals of Probability*, vol. 22, no. 4, pp. 2242-2274, 1994.

[11] A. Clark, P. Smith, and D. Taylor, "Instantaneous capacity of OFDM on Rayleigh-fading channels," *IEEE Trans. Inf. Theory*, vol. 53, no. 1, pp. 355-361, Jan. 2007.

[12] I.S. Gradshteyn, and I.M. Ryzhik, "Table of Integrals, Series and Products," *7th ed. New York Academic*, 2007.

[13] E. Kreyszig, "Advanced Engineering Mathematics," *9th ed. John Wiley & Sons*, New York, 2005.

[14] M. Tüchler, "Design of serially concatenated systems depending on the block length," *IEEE Trans. Comm.*, vol. 52, pp. 209-218, Feb. 2004.

Appendix A

Let $\mathbf{X}$ be a Gaussian vector with zero-mean and unit-variance. Further, let $f : \mathbb{R}^d \to \mathbb{R}$ be a measurable function with $E[f(\mathbf{X})^2] < \infty$. The Hermite rank $\nu(f)$ of f with respect to $\mathbf{X}$ is defined as [10]

$$\nu(f) \equiv \inf\Big\{\tau : \exists \text{ polynomial } P \text{ of degree } \tau \text{ with} \\ E\big[\big(f(\mathbf{X}) - E[f(\mathbf{X})]\big)P(\mathbf{X})\big] \neq 0\Big\}. \quad (38)$$

In the following, we show that the Hermite rank of $s_k\big(\tau_{c,q}, \tau_{s,q}\big)$ is at least 2. We basically follow the same derivation as in [11], where the Hermite rank of the sub-channel capacity as a function of the channel gains for an OFDM system has been calculated.

First, we show that $\nu(s_k) \neq 0$. Consider a zero-order polynomial $P(\mathbf{X}) = A_0$ with $\mathbf{X} = (X_1, X_2)$. Then, the condition in (38) becomes

$$\begin{aligned} &E\big[\big(s_k(\mathbf{X}) - E[s_k(\mathbf{X})]\big)P(\mathbf{X})\big] \\ &= A_0 E\big[s_k(\mathbf{X})\big] - A_0 E\big[s_k(\mathbf{X})\big] \\ &= 0, \end{aligned} \quad (39)$$

for all $A_0 \in \mathbb{R}$, and thus $\nu(s_k) \neq 0$. Next, consider a first-order polynomial $P(\mathbf{X}) = A_0X_1 + A_1X_2 + A_3$. Then, we have

$$\begin{aligned} &E\big[\big(s_k(\mathbf{X}) - E[s_k(\mathbf{X})]\big)P(\mathbf{X})\big] \\ &\quad = A_0E\big[X_1s_k(\mathbf{X})\big] + A_1E\big[X_2s_k(\mathbf{X})\big], \end{aligned} \tag{40}$$

where we have used the property $E[X_1] = E[X_2] = 0$. The random variables X_1 and X_2 are identically Gaussian distributed. Thus, we get

$$\begin{aligned} E\big[X_1s_k(\mathbf{X})\big] &= E\big[X_2s_k(\mathbf{X})\big] \\ &= \int_{-\infty}^{\infty}\int_{-\infty}^{\infty} x_1s_k(x_1,x_2)p(x_1,x_2)\mathrm{d}x_1\mathrm{d}x_2, \end{aligned} \tag{41}$$

where $p(x_1, x_2)$ is the joint probability function of the two correlated Gaussian random variables X_1 and X_2. Observe that $p(x_1, x_2)$ and $s_k(x_1, x_2)$ are even in (X_1, X_2). Thus, the integral in (41) is zero and it follows that $E\big[X_1s_k(\mathbf{X})\big] = E\big[X_2s_k(\mathbf{X})\big] = 0$, and therefore, $\nu(s_k) \neq 1$. We conclude that $\nu(s_k)$ is at least 2.

APPENDIX B

The covariance $\mathrm{Cov}\big[c_k(\kappa_0), c_k(\kappa_j)\big]$ between $c_k(\kappa_0)$ and $c_k(\kappa_j)$ for $1 \leq j \leq Q-1$ is given by

$$\mathrm{Cov}\big[c_k(\kappa_0), c_k(\kappa_j)\big] = \mathrm{E}[c_k(\kappa_0), c_k(\kappa_j)\big] - \mu_{S_k}^2, \tag{42}$$

where

$$\begin{aligned} \mathrm{E}[c_k(\kappa_0), c_k(\kappa_j)\big] = &\int_0^{\infty}\int_0^{\infty} \frac{1}{1+\rho_k x} \\ &\times \frac{1}{1+\rho_k y} f_{\kappa_0,\kappa_j}(x,y)\mathrm{d}x\mathrm{d}y. \end{aligned} \tag{43}$$

In (43), $f_{\kappa_0,\kappa_j}(x, y)$ is the joint PDF of κ_0 and κ_j, which follows a bivariate exponential distribution [9] with the form:

$$f_{\kappa_0,\kappa_j}(x,y) = \alpha \exp\big[-\beta(x+y)\big]\mathrm{I}_0\big(\theta\sqrt{xy}\big), \tag{44}$$

where

$$\alpha = \frac{1}{\eta^2(1-\delta_j)},\ \beta = \alpha\eta,\ \theta = 2\alpha\eta\sqrt{\delta_j}$$

and $\mathrm{I}_0(.)$ denotes the modified zero-order Bessel function of the first kind. We may substitute (44) into (43) to obtain

$$\begin{aligned} &\mathrm{E}[c_k(\kappa_0), c_k(\kappa_j)\big] \\ &= \alpha\int_0^{\infty}\int_0^{\infty} \frac{1}{1+\rho_k x}\frac{1}{1+\rho_k y}\exp\big[-\beta(x+y)\big] \\ &\times \mathrm{I}_0(\theta\sqrt{xy})\mathrm{d}x\mathrm{d}y \qquad (45) \\ &= \alpha\sum_{n=0}^{\infty}\left(\frac{\theta^{2n}}{4^n(n!)^2}\Big[\int_0^{\infty}\frac{x^n}{1+\rho_k x}\exp(-\beta x)\mathrm{d}x\Big]^2\right). \qquad (46) \end{aligned}$$

Note that (46) is obtained by using the series expansion of $\mathrm{I}_0(.)$ [12]. Using a substitution from [12], we may express the integral expression in (46) as

$$\begin{aligned} &\int_0^{\infty}\frac{x^n}{1+\rho_k x}\exp(-\beta x)\mathrm{d}x \\ &= \frac{(-1)^n}{\rho_k^{n+1}}\left[\exp\left(\frac{\beta}{\rho_k}\right)\mathrm{E}_1\left(\frac{\beta}{\rho_k}\right) + \sum_{s=1}^{n}(s-1)!\Big(-\frac{\rho_k}{\beta}\Big)^s\right]. \end{aligned} \tag{47}$$

Substituting (47) into (46), we get

$$\begin{aligned} \mathrm{E}[c_k(\kappa_0), c_k(\kappa_j)\big] = &\frac{\alpha}{\rho_k^2}\sum_{n=0}^{\infty}\left(\frac{\big(\frac{\theta}{2\rho_k}\big)^{2n}}{(n!)^2}\left[\exp\left(\frac{\beta}{\rho_k}\right)\mathrm{E}_1\left(\frac{\beta}{\rho_k}\right)\right.\right. \\ &\left.\left.+\sum_{s=1}^{n}(s-1)!\Big(-\frac{\rho_k}{\beta}\Big)^s\right]^2\right). \end{aligned} \tag{48}$$

Numerical calculations show that the series in (48) is rapidly convergent. The series representation (48) may therefore be used to efficiently calculate (42).